 https://doi.org/10.3311/PPme.41193

Periodica Polytechnica Mechanical Engineering, 69(3), pp. 252–258, 2025

Manufacturing Process of Laboratory Bipolar Plates Designed with Gas Flow Simulation

Erika Varga[1*], János Kelemen[1], Elek Kiss[1], Dávid István Kis[1], Attila Bata[1]

[1] Department of Innovative Vehicles and Materials, GAMF Faculty of Engineering and Computer Science, John von Neumann University, 10 Izsáki Street, H-6000 Kecskemét, Hungary
[*] Corresponding author, e-mail: varga.erika@nje.hu

Received: 04 June 2025, Accepted: 17 July 2025, Published online: 21 July 2025

Abstract

In present paper a low-resource-demanding targeted manufacturing technique is demonstrated for serpentine-structured bipolar plates (BPPs) for Proton Exchange Membrane Fuel Cell (PEMFC) test systems. In the phase of the technical design, Computational Fluid Dynamics (CFD) simulations were conducted to analyze the BPPs during continuous operation. The simulations revealed that the proposed 4-serpentine flow field with channel and land width of 1 mm and channel depth of 2 mm effectively distributes reactant gases across the active area of the Membrane Electrode Assembly (MEA), minimizing stagnant flow regions under operating conditions. The CFD simulations demonstrated that the flow channel design facilitated efficient water drainage, reducing the risk of water accumulation that could impede gas diffusion and decrease cell performance. Water mole fraction at the outlet was calculated to 0.3, while power dissipation density of the active areas reached homogeneously 5.4×10^{-3} W/m^3. BPPs with the appropriate structure were manufactured through a cost-efficient Wire Electrical Discharge Machining (WEDM) and Computer Numerical Control (CNC) milling technique highly appropriate for unique production of test cell components.

Keywords

bipolar plate, flow channels, CFD, milling

1 Introduction

Proton Exchange Membrane Fuel Cells (PEMFCs) have gained increasing attention as a clean and efficient energy conversion technology, particularly in transportation and portable power applications [1, 2]. Membrane Electrode Assemblies (MEAs) are the core units of the fuel cells, as they are responsible for the effective electrochemical reactions and the ion transfer required for the completion of chemical processes to produce electric energy from chemical energy. However, voltage obtained from a single MEA is moderate, thus MEAs are connected through bipolar plates (BPPs) in series in the fuel cell stacks. BPPs influence the performance, efficiency, and durability of PEMFCs, and serve multiple functions: distributing reactant gases, collecting current, and managing water and heat [3–6].

Among various flow field designs, the serpentine pattern is widely used due to its effective water removal and enhanced reactant distribution ability [7]. However, optimizing its geometry requires balancing manufacturing feasibility, pressure drop, and uniform flow distribution across the active area. Busqué et al. [8] demonstrated that the trapezoidal flow channel cross-section is more favorable than rectangular ones in the sense of current density, temperature and reaction rates. By Hajagos et al. [9] semi-circular channels on the anode side to improve hydrogen flow and U-shaped channels on the cathode side were developed for better hydrogen flow and water removal, respectively. Among rectangular channels, when stoichiometric ratio of hydrogen is 1.5, the standard type of BPP (land width = 0.75 mm, channel width = 1.05 mm) was proven to be the best, however, at increased stochiometric ratio the wider one, at which the hydrogen crossover also was significant, overperformed it [10]. Obstacles in the channels with different shapes influence the performance significantly, too [11].

To date, several types of materials, such as metals, graphite and advanced polymers have been developed for BPPs to ensure high electric and thermal conductivity as well as corrosion resistance [12, 13]. Material selection, however,

Cite this article as: Varga, E., Kelemen, J., Kiss, E., Kis, D. I., Bata, A. "Manufacturing Process of Laboratory Bipolar Plates Designed with Gas Flow Simulation", Periodica Polytechnica Mechanical Engineering, 69(3), pp. 252–258, 2025. https://doi.org/10.3311/PPme.41193

limits the reasonable manufacturing processes of these sophisticated components; in addition to the improved milling technologies, new concepts also have appeared such as micro-electrical discharge machining milling, rolling, EMF or laser-utilizing additive technologies [14–18]. Semi-stamp forming process was shown to improve the dimensional accuracy of the rubber forming process of serpentine channels [19], but double-step hydroforming process also can be feasible for complicated flow patterns [20].

This paper focuses on a low-resource-demanding manufacturing technology of serpentine-structured BPPs for self-developed fuel cell stacks including precision design, and presents Computational Fluid Dynamics (CFD) simulation to analyze gas flow behavior and water management to enhance targeted production. The insights gained aim to support the development of high-performance and cost-effective PEMFC test systems.

2 Modelling of the BPP flow channels

2.1 Composition of the fuel cell under study

Components of the fuel cell stack are presented in Table 1 and Fig. 1.

MEAs, electrochemically active parts of the cells are embedded between two BPPs, and the series is closed with closing plates, current collectors, isolating panels and endplates on both ends. Hydrogen is transferred to the anode side, while oxygen/air to the cathode side. This side of the BPPs are also responsible for the drainage of the product water. O-rings, fasteners, plate springs and cutting ring fittings are required for the stable assembly and gas tightness.

Table 1 Required components of the fuel cell

Component	Material/type	Number
Endplate	C45	2 pieces
Isolating panel	–	2 pieces
Current collector	Cu	2 pieces
Closing plate	1.2085	2 pieces
BPP	1.2085	No. MEAs + 2 pieces. In this case 2 × no. of MEAs + 2 pieces of half-plates.
MEAs	According to construction	According to construction
O-rings	NBR70	According to construction
Fasteners, socket head cap screw	M6 × 130	According to construction
Plate ring	Meusburger tool standard, d6.5/13 × 1.2	According to construction
Swagelok® fittings	SS-6M0-1-2	According to construction

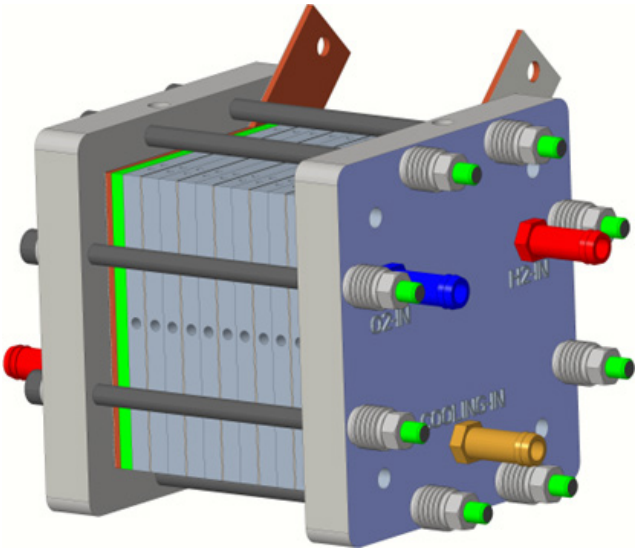

Fig. 1 Block chart of a fuel cell stack consisting of 5 MEAs

To simplify the manufacturing, two sides of the BPPs were manufactured in two separate plates, which were compressed to each other at their water cooling sides in the stack.

2.2 Software background for BPP modelling

COMSOL Multiphysics is a powerful simulation software [21] widely used in various scientific and engineering fields, including fuel cell modelling and simulation. This software allows users to study in detail the operation of fuel cells and optimize their performance. COMSOL Multiphysics allows simultaneous modelling and simulation of multiple physical phenomena, which is particularly important for fuel cells where thermal, flow and electrochemical processes are all involved. With the integrated Model Builder, users can easily create and manage models, including the definition of geometry, material properties and physical parameters. Its fuel cell module integrates the Navier-Stokes equations (for free flow) and the Darcy or Brinkman equations (for porous media flow) within a single simulation. This allows accurate modelling of situations where the fluid transitions between free and porous regions, as well as electrolyte data, characteristics of the electrochemical reaction kinetics, initial potential values, initial humidity and temperature values for gases are involved in simulating the working conditions of the whole fuel cell.

2.3 Model of the BPP in the single-cell stack

BPPs were designed with 4 serpentine channels of 1 mm width and 2 mm depth. The single cell model in Fig. 2 shows a model created in Creo Parametric CAD software [22]. The inflow channels and serpentine channels

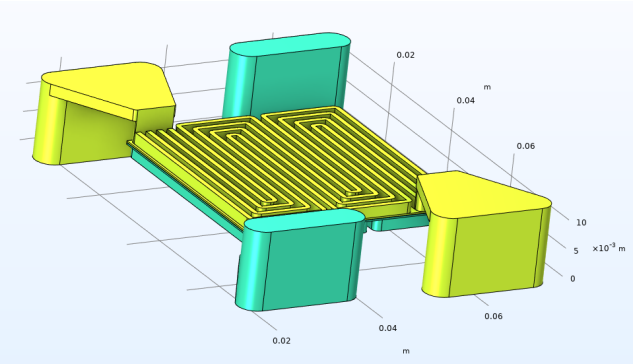

Fig. 2 Inverse model of the fuel cell with one MEA

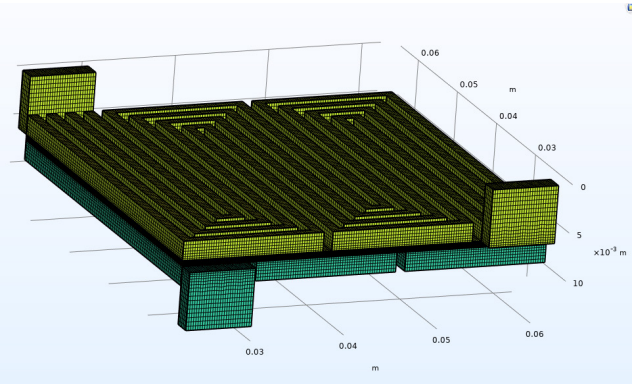

Fig. 4 Meshing in the fuel cell model

are the inverse of the real model, i.e., the flow channels in the BPPs appear solid in Fig. 2 and the air voids are the walls of the BPP.

To reduce the time required to run the model, a simplified model was created, in which the rounded edges of the flow channels have been eliminated, and instead of the complex geometry of the inflow channels, a simplified rectangular mesh has been integrated making meshing much easier, while not significantly affecting the accuracy of the calculations (Fig. 3). Deviations on the simulated polarization curves, the main indicators of the fuel cell performance, were below 3% at any point before and after simplification.

Rectangle meshing was applied to improve the meshing resource efficiency. On the different parts, meshing with different density was applied, depending on their thickness. A meshing generator called Edge was applied to create divisions within the boundaries, allowing to control, for example, the thickness of the membrane in terms of how many layers it should be sliced into (Fig. 4). The initial default meshing generated for the cell model was over 2 million elements, the simplified model is resolved to 650 thousand elements, greatly speeding up the simulations.

To simulate the gas distribution in the flow channels during stationary operation, fuel cell parameters have to be implemented and specified for each system. Expected parameters of the MEAs to be applied later in the laboratory tests are summarized in Table 2. Power dissipation at the MEA is depicted in Fig. 5.

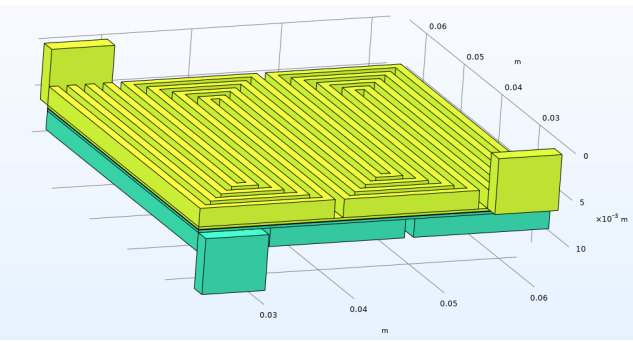

Fig. 3 Simplified model of the fuel cell

High-density regions in Fig. 5 appear at the gas flow channels thanks to the active electrochemical reactions. Apart from the edges, there are no low-energy regions within the horizontal plane, indicating the homogeneous distribution of reaction sites, which is the result of the appropriate gas transport in the BPPs.

Table 2 Fuel cell parameters applied during the gas flow simulations

Parameter	Measure	Unit
GDL thickness[1]	2.1×10^{-4}	m
Porous electrode thickness[1]	2.125×10^{-4}	m
Membrane thickness[1]	2.75×10^{-5}	m
GDL porosity[1]	2.10	–
Catalyst layer electrolyte (ionomer) volume fraction[1]	0.25	–
Catalyst layer pore volume fraction[1]	0.30	–
GDL permeability[1]	1.9×10^{-12}	m^2
Catalyst layer permeability	10^{-14}	m^2
GDL conductivity[1]	125.00	S/m
Membrane conductivity[1]	5	S/m
Cell temperature[2]	353.15	K
Reference pressure[2]	10133×10^5	Pa
Cell voltage[2]	0.4	V
Reference exchange current density, cathode	0.001	A/m^2
Reference exchange current density, anode	100	A/m^2
Transfer coefficient cathode	0.5	–
Specific surface area	1×10^7	1/m
Humidification temperature[2]	65 °C	K
Anode stochiometry[2]	1.5	–
Cathode stochiometry (operation in air)[2]	1.3	–
Hydrogen back pressure[2]	3.5	bar
Oxygen back pressure[2]	3.3	bar

[1] Goal parameters of the MEA under development.
[2] Proposed test parameters of the fuel cell under development.
Unmarked data were implemented from the demo data set of COMSOL Multiphysics [21].

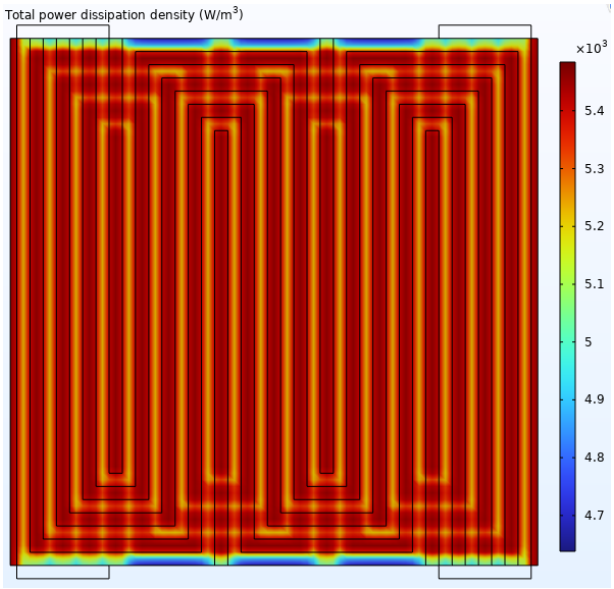

Fig. 5 Total power dissipation density (W/m³) at operation at 0.4 V

At the cathode side the distribution of the product water in the BBP channels is an indication of the reaction and material transport efficiency. In Fig. 6 on the cathode side BPP channels water mole fraction increases continuously from 0 to 0.25–0.30 at the outlet, without water traps. In these circumstances water transfer is effective, and flooding of the MEA can be avoided [23, 24].

In Figs. 7 and 8 continuous hydrogen and oxygen mol fraction decrease can be observed, which is evidence of the effective gas flow in the channels.

Based on the CFD results on the flow channel design, BPP with composition depicted in Fig. 9 was developed.

3 Manufacturing

3.1 Material selection

For BPP material corrosion resistant and magnetizable steel was selected to enhance processability with grade of

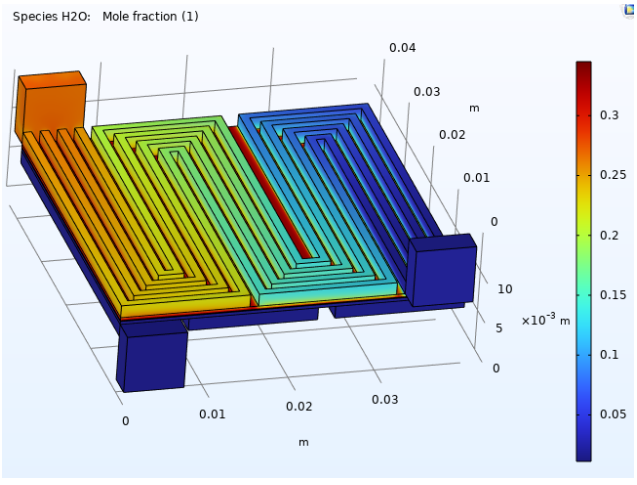

Fig. 6 Water mole fractions at the cathode side at operation at 0.4 V

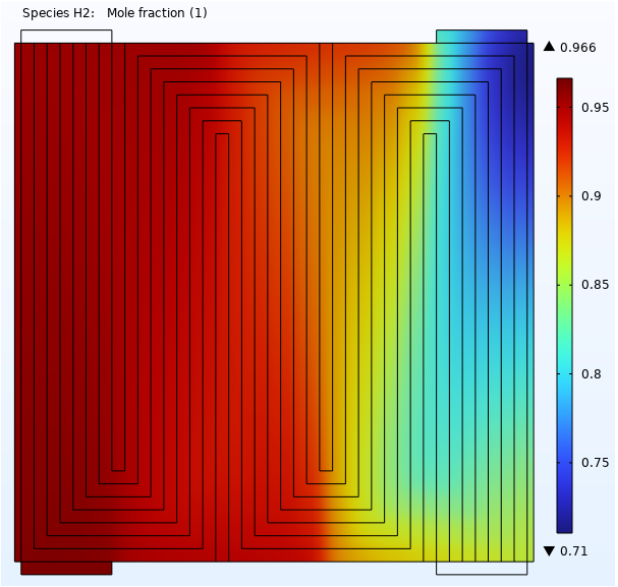

Fig. 7 Hydrogen mol fraction at the anode side at operation at 0.4 V

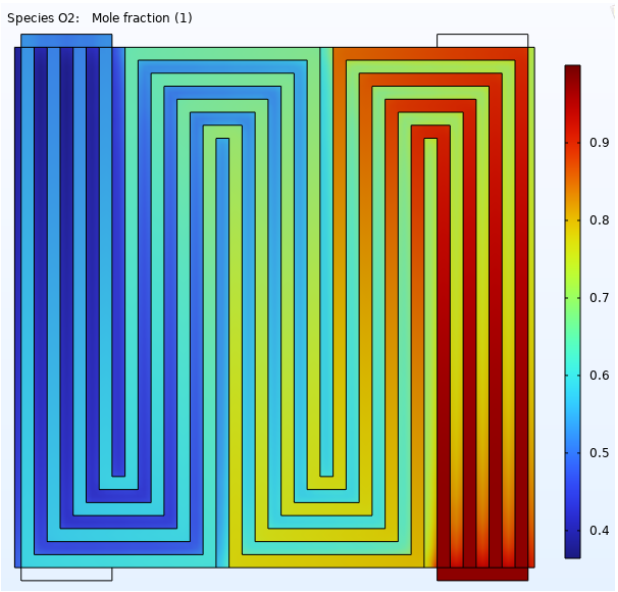

Fig. 8 Oxygen mol fraction at the cathode side at operation at 0.4 V

1.2085, which has high chromium content, but characterized by a ferritic structure. This type of tool steel (from standard parts of suppliers) is stress relieved.

It is important that the internal stresses released during machining do not cause significant warpage. To achieve the desired surface roughness and flatness-parallelism, the machining of the plates was completed by surface grinding, which required clamping on a magnet table. Hung et al. [25] demonstrated that in case of die-sinking micro-electrical discharge machining the increment in the material removal increased the surface roughness, the effect of which on the cell performance was not obvious probably due to the large channel depth (600 mm). In our case roughness after grinding was appropriate.

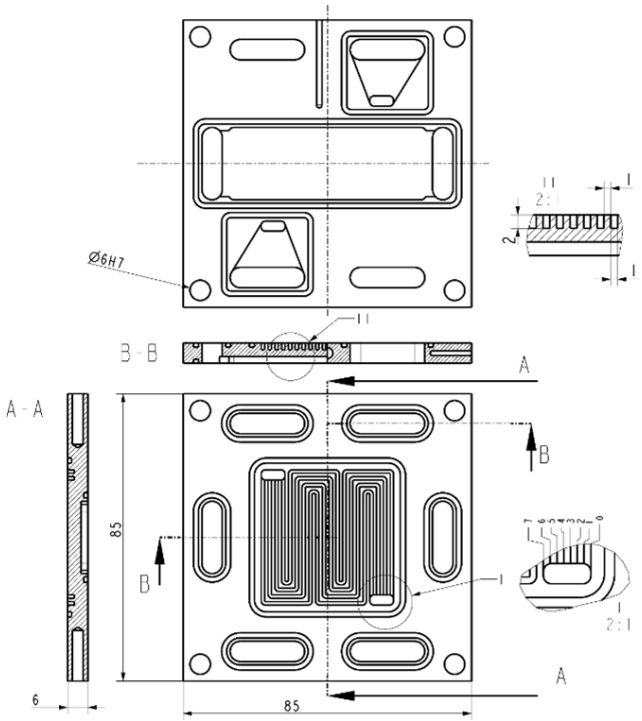

Fig. 9 Drawing of the BPP

3.2 Selection of machining tools

All connection plates in fuel cells should be designed with identical reference holes for easy and accurate gripping and resetting, which also help to ensure accurate connections during assembly. After cutting and setting the uniform sheet sizes, 4 (corner) d6H7 reference holes are made in each plate by WEDM (Wire Spark Machining) with a Fanuc Tape Cut-W2 instrument. The same concept was used for gas and water inlets and outlets.

CNC milling and drilling using a TOS FV30 NCT100 device was choosen for fine processing. There are operations on both sides of the plate, so a clamping device had to be manufactured to ensure that the base is always maintained after milling.

During clamping, two grinded shoulder screws were used diagonally at the corners to ensure H7/g6 fit quality and hold in position (Fig. 10). The other generic screws were responsible for pulling the plates down. The center screws are removed and installed in a programmed manner, depending on where the milling is taking place. After the programmed M00 (program run stop), they are installed or removed or reassembled to ensure no collisions.

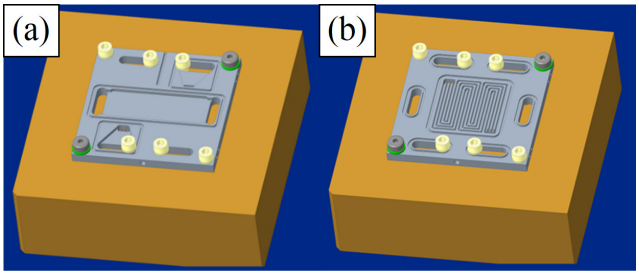

Fig. 10 BPP clampig for CNC milling, matched shoulder bolts with clamping screws: (a) water cooling side, (b) serpentine side

Small milling tools should be used in case of the grooves, pockets and their corner radii. This makes production more difficult because very high speeds are required. List of the carbide tools chosen: BR55-4E-010, BR55-4E-015, BR55-4E-030. Tool paths are presented in Fig. 11.

The selected methodology, taking into account the machine capability and tooling target tool diameter (d), depth of cut (a_z), radial depth of cut (a_e), feed rate (F), number of revolutions (S) is detailed in Table 3.

A 0.2 mm/side allowance was applied during all milling operations to allow for the final operation of surface grinding to adjust the proper surface roughness, which is important for the sealing of the MEA electrode assembly. The O-ring groove depths were set to 0.2 mm sealing tightness. Products are depicted in Fig. 12.

4 Conclusions

BPPs are critical components of the fuel cells due to their gas and water distribution role. In this study flow channel structure was simulated to assess the behavior of the BPP under working. The designed component was then manufactured by conventional WEDM a CNC milling, the

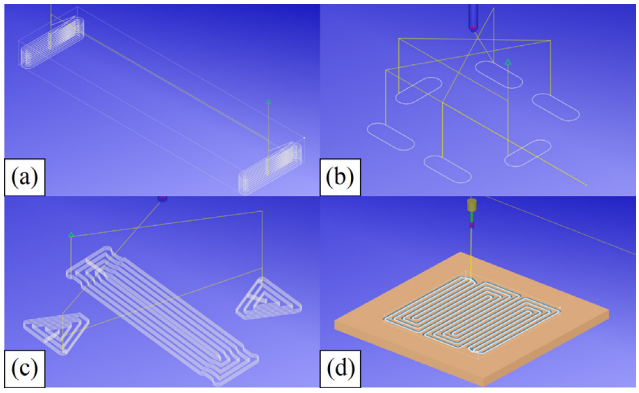

Fig. 11 Tool paths: (a) for water passage (b) for O-ring grooves around passages, (c) for the gas transfer and cooling pocket, (d) for the serpentine channels

Table 3 Applied milling parameters: tool diameter (d), depth of cut (a_z), radial depth of cut (a_e), feed rate (F) and RPM (S)

d (mm)	a_z (mm)	a_e (mm)	F (mm/min)	S (1/min)
1.0	0.05	0.3 × d	50	8000
1.5	0.1	0.4 × d	80	6000
3.0	0.2	0.6 × d	120	4000

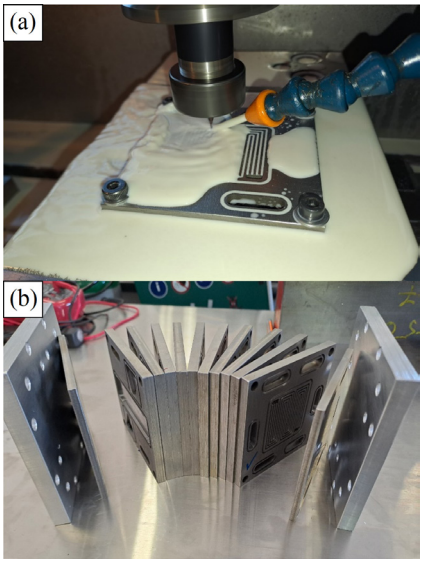

Fig. 12 Workshop activities: (a) production process, (b) finalized BPPs with end plates

process of which is detailed to demonstrate an affordable solution for unique BPP production for test systems.

Acknowledgement

This work was supported by National Laboratory for Renewable Energy (Project no. RRF-2.3.1-21-2022-00009), that has been implemented with the support provided by the Recovery and Resilience Facility of the European Union within the framework of Programme Szechenyi Plan Plus, Hungary.

References

[1] Kun, K., Szabó, L., Varga, E., Kis, D. I. "Development of a Hydrogen Fuel Cell Prototype Vehicle Supported by Artificial Intelligence for Green Urban Transport", Energies, 17(7), 1519, 2024. https://doi.org/10.3390/en17071519

[2] Wang, Z., Liu, Z., Fan, L., Du, Q., Jiao, K. "Application progress of small-scale proton exchange membrane fuel cell", Energy Reviews, 2(2), 100017, 2023. https://doi.org/10.1016/j.enrev.2023.100017

[3] Tang, A., Crisci, L., Bonville, L., Jankovic, J. "An overview of bipolar plates in proton exchange membrane fuel cells", Journal of Renewable and Sustainable Energy, 13(2), 022701, 2021. https://doi.org/10.1063/5.0031447

[4] Chen, X., Chai, F., Hu, S., Tan, J., Luo, L., Xie, H., Wan, Z., Qu, Z. "Design of PEMFC bipolar plate cooling flow field based on fractal theory", Energy Conversion and Management: X, 20, 100445, 2023. https://doi.org/10.1016/j.ecmx.2023.100445

[5] Zhao, T., Jiang, K., Fan, W., Lu, D., Zheng, D., Cui, H., Yang, L., Lu, G., Liu, Z. "Nature-inspired hybrid wettability surface to enhance water management on bipolar plates of PEMFC", Chemical Engineering Journal, 466, 143288, 2023. https://doi.org/10.1016/j.cej.2023.143288

[6] Lee, S., Jeong, H., Ahn, B., Lim, T., Son, Y. "Parametric study of the channel design at the bipolar plate in PEMFC performances", International Journal of Hydrogen Energy, 33(20), pp. 5691–5696, 2008. https://doi.org/10.1016/j.ijhydene.2008.07.038

[7] Wilberforce, T., Amiri, A. "Comparative study on bipolar plate geometry designs on the performance of proton exchange membrane fuel cells", Fuel, 346, 128389, 2023. https://doi.org/10.1016/j.fuel.2023.128389

[8] Busqué, R., Bossio, M., Brigido, A., Lara, A. "Effects of Different Channel Geometries of Metallic Bipolar Plates on Proton Exchange Membrane Fuel Cell Performance", Energies, 16(23), 7702, 2023. https://doi.org/10.3390/en16237702

[9] Hajagos, S., Kovács, J. G. "Polymer-based Bipolar Plates for Fuel Cells: Design, Simulation, and Manufacturing", Periodica Polytechnica Mechanical Engineering, 69(1), pp. 40–45, 2025. https://doi.org/10.3311/PPme.38589

[10] Jung, A., Kong, I. M., Baik, K. D., Kim, M. S. "Crossover effects of the land/channel width ratio of bipolar plates in polymer electrolyte membrane fuel cells", International Journal of Hydrogen Energy, 39(36), pp. 21588–21594, 2014. https://doi.org/10.1016/j.ijhydene.2014.06.052

[11] Çelik, S., Yagiz, M., Yildirim, F., Topcu, A. "Experimental study on the flow field geometry of the PEM fuel cell bipolar plates: The effects of various shaped blocks embedded in serpentine pattern on cell performance", Fuel, 358, 130202, 2024. https://doi.org/10.1016/j.fuel.2023.130202

[12] Kakati, B. K., Mohan, V. "Development of Low-Cost Advanced Composite Bipolar Plate for Proton Exchange Membrane Fuel Cell", Fuel Cells, 8(1), pp. 45–51, 2008. https://doi.org/10.1002/fuce.200700008

[13] Zhang, P. C., Han, Y. T., Shi, J. F., Li, T., Wang, H. Y., Wang, X. Y., Sun, J. C. "ZrC Coating Modified Ti Bipolar Plate for Proton Exchange Membrane Fuel Cell", Fuel Cells, 20(5), pp. 540–546, 2020. https://doi.org/10.1002/fuce.201900241

[14] Bauer, A., Härtel, S., Awiszus, B. "Manufacturing of Metallic Bipolar Plate Channels by Rolling", Journal of Manufacturing and Materials Processing, 3(2), 48, 2019. https://doi.org/10.3390/jmmp3020048

[15] Huang, P., Chen, Z., Zhang, J., Wu, M., Liu, Y., Zhang, F., Chen, Y., Chen, X. "Stainless steel bipolar plate fuel cell with different flow field structures prepared by laser additive manufacturing", International Journal Heat Mass Transfer, 183, 122186, 2022. https://doi.org/10.1016/j.ijheatmasstransfer.2021.122186

[16] Hung, J.-C., Yang, T.-C., Li, K. "Studies on the fabrication of metallic bipolar plates—Using micro electrical discharge machining milling", Journal of Power Sources, 196(4), pp. 2070–2074, 2011. https://doi.org/10.1016/j.jpowsour.2010.10.001

[17] Sánchez-Molina, M., Amores, E., Rojas, N., Kunowsky, M. "Additive manufacturing of bipolar plates for hydrogen production in proton exchange membrane water electrolysis cells", International Journal of Hydrogen Energy, 46(79), pp. 38983–38991, 2021. https://doi.org/10.1016/j.ijhydene.2021.09.152

[18] Rahiman, M. A. K., Murugasen, P. K., Karibeeran, S. S. "Fabrication of Metallic Bipolar Plate for Proton Exchange Membrane Fuel Cell Using Electromagnetic Forming Technique", Fuel Cells, 25(2), e70004, 2025. https://doi.org/10.1002/fuce.70004

[19] Elyasi, M., Ghadikolaee, H. T., Hosseinzadeh, M. "Investigation of dimensional accuracy in forming of metallic bipolar plates with serpentine flow field", The International Journal of Advanced Manufacturing Technology, 96(1), pp. 1045–1060, 2018. https://doi.org/10.1007/s00170-018-1650-5

[20] Mohammadtabar, N., Bakhshi-Jooybari, M., Hosseinipour, S. J., Gorji, A. H. "Feasibility study of a double-step hydroforming process for fabrication of fuel cell bipolar plates with slotted interdigitated serpentine flow field", The International Journal of Advanced Manufacturing Technology, 85(1), pp. 765–777, 2016. https://doi.org/10.1007/s00170-015-7960-y

[21] COMSOL Inc. "COMSOL Multiphysics, (Version 6.2)", [computer program] Available at: https://www.comsol.com/release/6.2 [Accessed: 01 March 2025]

[22] PTC Inc. "Creo Parametric, (Version 11.0.3.0)", [computer program] Available at: https://www.ptc.com/en/products/creo/parametric [Accessed: 01 March 2025]

[23] Benkovic, D., Fink, C., Iranzo, A. "Qualitative and quantitative determination of liquid water distribution in a PEM fuel cell", International Journal of Hydrogen Energy, 52, pp. 1360–1370, 2024. https://doi.org/10.1016/j.ijhydene.2023.09.161

[24] Zhang, Y., Tu, Z. "Flow-field design of the bipolar plates in polymer electrolyte membrane fuel cell: Problem, progress, and perspective", Applications in Energy and Combustion Science, 17, 100244, 2024. https://doi.org/10.1016/j.jaecs.2023.100244

[25] Hung, J.-C., Chang, D.-H., Chuang, Y. "The fabrication of high-aspect-ratio micro-flow channels on metallic bipolar plates using die-sinking micro-electrical discharge machining", Journal of Power Sources, 198, pp. 158–163, 2012. https://doi.org/10.1016/j.jpowsour.2011.09.065